STUDY ON THE EFFECT OF ASH LAYER ON FLOW AND HEAT TRANSFER IN DIESEL PARTICULATE FILTER BASED ON 3-D THERMAL LATTICE BOLTZMANN METHOD

by

Xiangdong LI, Tiechen ZHANG, and Xiaori LIU*

Hebei Key Laboratory of Thermal Science and Energy Clean Utilization,
School of Energy and Environmental Engineering, Hebei University of Technology,
Tianjin, China

Original scientific paper
https://doi.org/10.2298/TSCI221109052L

After the Diesel engine works for a long time, dense ash layer will be formed on the diesel particulate filter surface, which will increase the back pressure on the diesel particulate filter surface and seriously affect the normal operation of the diesel particulate filter. The diesel particulate filter micro-structure is generated by 3-D reconstruction technology. Moreover, the particle layer and ash layer are reconstructed by quartet structure generation set. The exhaust gas with a velocity of 0.05-0.25 m/s is introduced into the diesel particulate filter model. Under the condition of 873 K temperature field, the 3-D lattice Boltzmann method is used to explore the influence of the particle layer and ash layer accumulated in its micro-structure on its flow and heat transfer. The results show that with the accumulation of ash, the flow velocity in the diesel particulate filter increases with the decrease of porosity. The existence of ash layer increases the pressure difference between the inlet and outlet of the structure, and the pressure difference between the inlet and outlet of the structure increases with the increase of the air inlet speed. Under the same flow conditions, the heat transfer process of structures containing ash stratification is faster, and the highest temperature point moves forward accordingly. This has certain guiding significance for exploring the thermal load of ash containing diesel particulate filter structure.

Key words: *diesel particulate filter, lattice Boltzmann method, ash, micro porous medium structure, flow heat transfer*

Introduction

At present, Diesel engine is the main power source of medium and large vehicles, and its good combustion power, durability and reliability are sought after by people [1]. However, the exhaust particulate matter produced by diesel engine is also a main cause of particulate pollution and haze formation in the atmospheric environment [2]. Diesel particulate filter (DPF) is an effective means to deal with diesel exhaust emission. As shown in fig. 1, the DPF system achieves the acquisition of particulate matter (PM) in the exhaust through the porous wall, and the filtration efficiency of the fine PM can reach 95%, and the filtration efficiency of the fine PN can reach 99% [3]. The DPF has become a routine and effective way to deal with PM and emission regulations in recent years. However, with the long-term operation of DPF, large quantity of ash accumulate on the wall of DPF, resulting in the increase of DPF back pressure,

* Corresponding author, e-mail: happylxrshanda@163.com

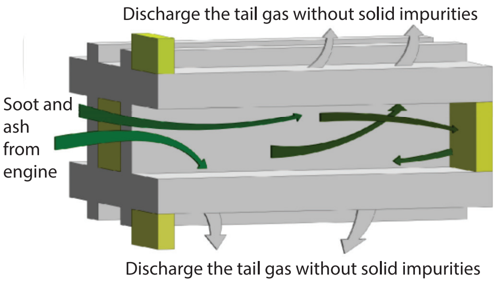

Figure 1. The DPF channel structure

which seriously affects the work and service life of DPF [4]. Therefore, it is particularly important to study the influence of ash layer on DPF operation. Normally, the use of post injection, fuel burner or electric heater at the DPF entrance can raise the temperature to 550 °C or more, which should be regenerated [5, 6]. The study shows that [5, 7]: active regeneration has increased by 2-3 orders of magnitude compared with that of DPF export particulates without regeneration. Therefore, in order to better show the impact of accumulated ash layer and particulate layer on DPF, the simulation of this paper applies active regeneration conditions.

Ash is mainly derived from lubricating oil in Diesel engines. The ash produced in lubricating oil reaches more than 90% of the integral part of ash. Ash is generally composed of elements such as Ca, Mg, P, and S. Under the influence of chemical elements, the shape and color of ash layer will also be changed [4]. Regardless of DPF active regeneration, passive regeneration and active passive hybrid regeneration, dense ash layer structure will be formed on the DPF wall after long-term operation of DPF. As shown in fig. 2, the process of generating ash layering in DPF can be divided into three-stages: surface transition section, ash filter cake section and ash blockage section. This paper simulates the later stage when a large amount of ash accumulates on the wall of the duct, that is, the ash blocking section. By observing the micro-structure of ash, it can be found that the ash layered structure is also a porous medium with extremely irregular pores [8]. At present, the best way to test the oxidation and production of particulate PM is to apply thermogravimetric analysis experiment [9]. The optimum oxidation temperature of non-combustible materials is at 400-570 °C. Generally, the ash layer, particulate layer and DPF structure are expressed in nm level. For DPF wall, its micro-structure also has the characteristics of porous media [10].

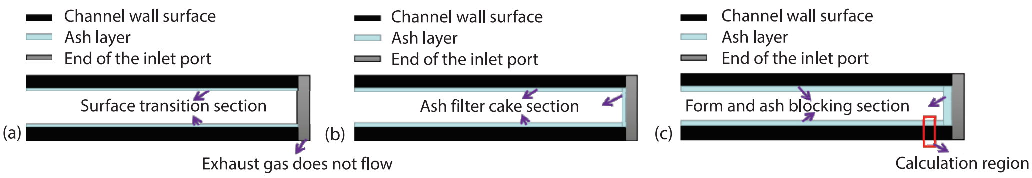

Figure 2. The accumulation process of ash in DPF; (a) surface transition section, (b) ash filter cake section, and (c) ash blockage section [8]

The lattice Boltzmann method (LBM) is a method that simulates heat and mass transport processes between macro and micro scales [11]. It does not need to consider the motion of a single particle, but regards the motion of all particulates as a whole. It has the advantages of micro method and macro method, and is easier to be used in the calculation of complex geometric fields. The LBM was applied to the flow and heat transfer calculation of 3-D micro DPF wall, which not only save calculation resources, but also improved the calculation accuracy [12]. The D_2Q_9 model (2-D nine velocity vectors model) in LBM was used to simulate the flow in cordierite DPF. It was found that the pressure distribution depended on the heterogeneity of pore structure. Secondly, computed tomography (CT) scanning technology and D_3Q_{15} model (3-D fifteen velocity vectors model) were used to simulate the 3-D soot oxidation process [13]. Then, the ash particles were introduced into LBM, which confirmed the blocking effect of ash particles on DPF when only considering the heat transfer from DPF to solid wall [14]. In the research, it was found that when the temperature was higher than 700 K, the chemical reaction rate was greatly improved, and the regeneration efficiency was greatly accelerated [15]. Li *et al.* [16] introduced the DDLB-CA model in LBM into DPF to simulate the generation process of bridge structure in 2-D DPF micro-structure. It was confirmed that the smaller the air-flow velocity is, the earlier the bridge structure was formed. On the basis of previous studies, it can be found that:

– There are still deficiencies in the research on the exhaust process of DPF blocked by ash layer.
– The blocking degree of ash layer to DPF and the range of increasing back pressure of DPF need to be studied.
– The LBM is used to simulate 3-D micro DPF, but there are still few studies on the flow and heat transfer process with the coexistence of ash layer and particle layers.
– The study of characterizing the micro morphology of ash layer and particle layers in DPF still needs to be improved.

To sum up: using 3-D LBM to combine the porous media layer after the deposition of ash and particles with the micro-structure of DPF is particularly valuable for studying the flow and heat transfer process in DPF and the influence of ash on DPF exhaust.

In this paper, the micro-structure of DPF was reconstructed by CT scanning. The quartet structure generation set (QSGS) is used to characterize the micro morphology and randomness of ash layer and particle layers. At the same time, combined with the 3-D LBM method, the porous medium layer after ash and particle deposition is combined with the micro-structure of DPF to explore the exhaust gas-flow after non-combustible ash layer accumulated on the micro wall of DPF in the process of active regeneration, and calculate the process of flow coupled heat transfer in DPF. This is of great help to study the blocking factors of ash layer on DPF exhaust when particle layers and ash layer coexist in the process of DPF exhaust.

Lattice Boltzmann calculation method

Lattice Boltzmann-Bhatnagar, Gross and Krook method

The equilibrium distribution function equation, density distribution equation and temperature distribution equation of lattice Boltzmann equation are established:

$$f_\alpha\left(x+\Delta x, t+\Delta t\right)-f_\alpha\left(x,t\right)=-\frac{1}{\tau+0.5}\left(f_\alpha+f_\alpha^{\mathrm{eq}}\right)\Big|_{(x,t)} \tag{1}$$

$$g_\alpha\left(x+\Delta x, t+\Delta t\right)-g_\alpha\left(x,t\right)=-\frac{1}{\tau+0.5}\left(g_\alpha+g_\alpha^{\mathrm{eq}}\right)\Big|_{(x,t)} \tag{2}$$

where α is the distribution direction of particulates, x – the position of the distribution function, Δt – the time step, τ – the dimensionless relaxation time, f_α – the density distribution function, f_α^q – the equilibrium density distribution function, g_α – the temperature distribution function, and g_α^q – the equilibrium temperature distribution function.

The D_3Q_{19} lattice model is adopted in this paper, and its model structure is shown in the fig. 3. Its discrete velocity e_α:

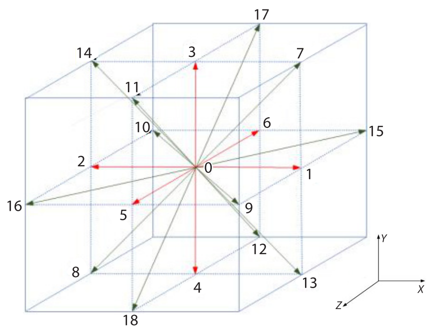

Figure 3. The D_3Q_{19} lattice model

$$e_\alpha = \begin{Bmatrix} 0,1,-1,0,0,0,0,1,-1,1,-1,0,0,1,-1,1,-1,0,0 \\ 0,0,0,1,-1,0,0,1,-1,0,0,1,-1,-1,1,0,0,1,-1 \\ 0,0,0,0,0,1,-1,0,0,1,-1,1,-1,0,0,-1,1,-1,1 \end{Bmatrix} \tag{3}$$

The corresponding weight coefficient w_α is:

$$w_\alpha = \begin{Bmatrix} 1/3\left|\vec{e}_\alpha = 0\right| \\ 1/18\left|\vec{e}_\alpha = 1\right| \\ 1/36\left|\vec{e}_\alpha = \sqrt{2}\right| \end{Bmatrix} \tag{4}$$

Zou-He boundary is used to calculate velocity distribution function and temperature distribution function at inlet and outlet. However, for 3-D models, Zou-He boundary cannot be assumed for unknown velocity, pressure and temperature boundary. The non-equilibrium extrapolation function [17] is introduced, which is a distribution equation with second-order accuracy. The principle is:

$$f_\alpha^{-1} = 2f_\alpha^0 - f_\alpha^1 \tag{5}$$

where $f_\alpha^{-1}, f_\alpha^0$, and f_α^1 are the distribution functions at the virtual boundary lattice points, the real boundary lattice points and the adjacent boundary lattice points, respectively.

For the velocity boundary, the velocity at the initial time of the boundary u_0 is known, but the density on the boundary ρ_0 is unknown. For the pressure boundary, the pressure at the boundary P_1 is known and the velocity at the boundary u_1 is unknown. Therefore, the adjacent lattice points are used to replace the operation lattice points. The non-equilibrium extrapolation equation is introduced to obtain:

The non-equilibrium extrapolation equation of the velocity boundary:

$$f_\alpha^{\mathrm{eq}} = w_\alpha \left\{\rho_1 + \rho_0\left[1 + 3e_\alpha u_0 + 4.5(e_\alpha u_0)^2 - 1.5u_0^2\right]\right\} \tag{6}$$

The non-equilibrium extrapolation equation of the pressure boundary:

$$f_\alpha^{\mathrm{eq}} = w_\alpha \left\{\frac{p1}{C_s^2} + \rho_0\left[1 + 3e_\alpha u_1 + 4.5(e_\alpha u_1)^2 - 1.5u_1^2\right]\right\} \tag{7}$$

In the calculation of flow process and heat transfer process, both eqs. (1) and (2) need to go through the process of collision and migration. The corresponding collision and streaming steps are:

Collision steps when calculating density distribution function:

$$\tilde{f}_\alpha\left(x, t+\Delta t\right) - f_\alpha(x,t) = -\frac{1}{\tau + 0.5}\left(f_\alpha + f_\alpha^{\mathrm{eq}}\right)\Big|_{(x,t)} \tag{8}$$

Streaming steps when calculating density distribution function:

$$f_\alpha(x + \Delta x, t + \Delta t) = \tilde{f}_\alpha(x, t + \Delta t) \tag{9}$$

Collision steps for calculating temperature distribution function:

$$\tilde{g}_\alpha\left(x, t+\Delta t\right) - g_\alpha(x,t) = -\frac{1}{t + 0.5}\left(g_\alpha + g_\alpha^{\mathrm{eq}}\right)\Big|_{(x,t)} \tag{10}$$

Streaming steps for calculating temperature distribution function:

$$g_\alpha(x+\Delta x, t+\Delta t) = \tilde{g}_\alpha(x, t+\Delta t) \tag{11}$$

where $\tilde{f}$ and $\tilde{g}$ are the state functions of density and temperature after collision, respectively.

In the calculation of DPF, the distribution function is used to characterize its macroscopic flow properties:

$$\rho = \sum_\alpha f_\alpha,\ P = C_s^2 \rho,\ \sum_\alpha e_\alpha f_\alpha \tag{12}$$

where the lattice sound velocity C_s^2 is 1/3.

Model and boundary conditions

Combined with the 3-D flow and heat transfer problem, the calculation accuracy is considered. In this paper, the non-equilibrium extrapolation form of Zou-He velocity boundary is applied at the inlet, and a constant pressure is applied at the outlet. This ensures the stability of fluid-flowing in the flow field and structure at the outlet. The non-equilibrium extrapolation form of bounces is applied around the boundary to ensure its convergence. The DPF structure is internally applied with no slip bounces. In terms of heat transfer, set the inlet temperature to 873 K and the outlet temperature to 773 K. It is surrounded by a periodic boundary. The physical conditions are shown in fig. 4.

Considering the stacking sequence of particle layers and ash layer on the DPF structure, and combination with the reference length, 6 layers of particle layers and 24 layers of DPF Structure I, and 5 layers of particle layers, 1 layer of ash layer and 24 layers of DPF Structure II. Boundary conditions are applied to Structures I and II and they are set as the control group, the porosity ε of ash layer is 0.49. Their structural models are shown in fig. 5.

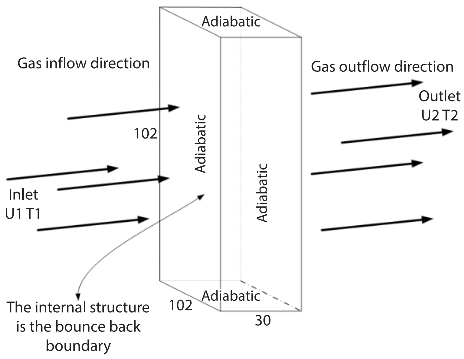

Figure 4. The DPF flow and heat transfer model of DPF wall

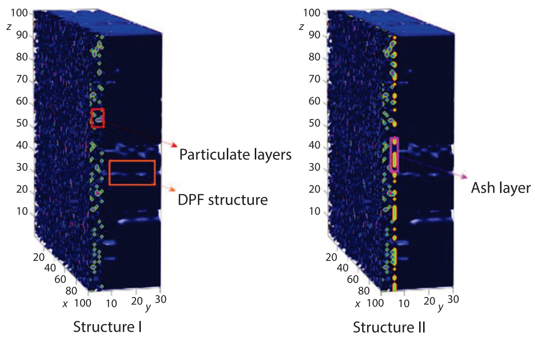

Figure 5. The physical model with 0 and 1 ash layer added

Parameter and structure construction

Structure construction

With regard to the micro morphology structure of DPF wall, CT scanner is used to scan and obtain 3-D reconstruction structure. The micro-structure of DPF obtained by CT scanner is shown in fig. 6. The DPF parameters obtained are: density ρ = 2100 kg/m^3, thermal conductivity λ = 2.5 W/ms, constant pressure specific heat C_p = 840 J/kgK, thermal diffusion coefficient $\alpha = 1.42 \cdot 10^{-6}$ m^2/s, porosity ε = 0.5216, and wall thickness $\delta = 4.716 \cdot 10^{-4}$ m.

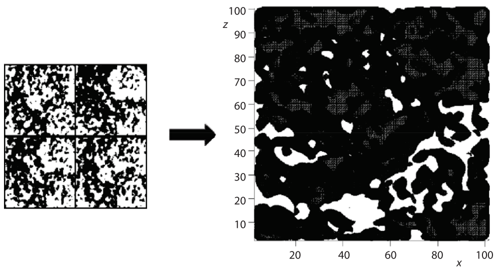

Figure 6. The 3-D reconstructed DPF structure

Quartet structure generation set can effectively characterize the randomness of porous media structure, and can be used to characterize the randomness of ash layer and particulate layers. The ash layer and particulate layers are shown in figs. 7 and 8. The parameters selected for the particle layer are [18, 19]: density ρ = 100 kg/m^3, thermal conductivity λ = 0.108 W/ms, constant pressure specific heat C_p = 1510 J/kgK, thermal diffusion coefficient $\alpha = 7.15 \cdot 10^{-7}$ m^2/s, porosity $\varepsilon = 0.95$, and wall thickness δ is $9.825 \cdot 10^{-5}$ m. The parameters selected for ash layer are [20, 21]: density ρ = 130 kg/m^3, thermal conductivity λ = 0.14 W/ms, constant pressure specific heat C_p = 1800 J/kgK, thermal diffusion coefficient $\alpha = 5.98 \cdot 10^{-7}$ m^2/s, porosity $\varepsilon = 0.49$, and wall thickness $\delta = 1.965 \cdot 10^{-5}$ m.

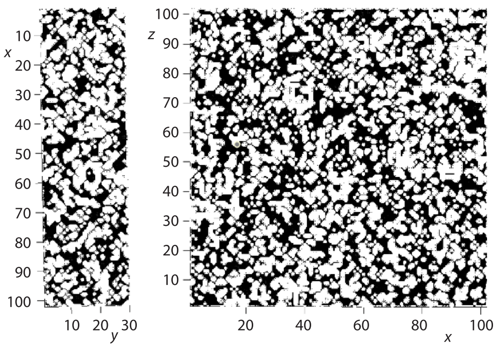

Figure 7. Ash layer generated by QSGS

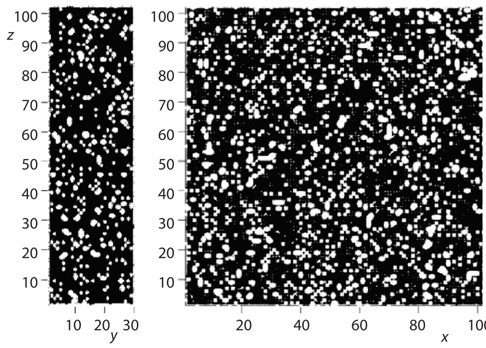

Figure 8. particulate layer generated by QSGS

Permeability of porous media

Combined with Darcy's law, the calculation formula of porous medium permeability under lattice unit is derived [22]:

$$K = -\frac{\mu\langle u_x \rangle}{\nabla P} = \frac{\rho v}{C_s^2 \Delta\rho} \frac{1}{NxNyNz} \sum_{i=1}^{Nx} \sum_{j=1}^{Ny} \sum_{k=1}^{Nz} u_x(i,j,k) \tag{13}$$

where v is the dynamic viscosity under the unit of fluid lattice, $\langle u_x \rangle$ – the average velocity in the x direction, $\Delta\rho$ – the difference of import and export density, and Nx, Ny, and Nz are the three directions of x, y and z.

According to the aforementioned eq. (13), the permeability of DPF structure on CT scan surface can be obtained, and its value is $7.14 \cdot 10^{-12}$ m^2. The permeability of the generated ash layer is $2.81 \cdot 10^{-13}$ m^2. The permeability of the particulate layers can also be calculated to be $4.13 \cdot 10^{-14}$ m^2.

Unit conversion

The reference length in this paper is defined as the accuracy of the CT scanner, that is $lr = 1.965 \cdot 10^{-5}$ m, Pr = 0.677, gas density ρ = 0.64 kg/m^3, and dynamic viscosity $\mu = 3.04 \cdot 10^{-5}$ kg/ms. Its calculation parameters are shown in tab. 1.

Table 1. Conversion between physical units and grid units

Physical unit	Physical scale	Lattice unit	Lattice scale
Computational domain length, L	$2.0043 \cdot 10^{-3}$ m	Lb	102
Computational domain width, W	$2.0043 \cdot 10^{-3}$ m	W_b	102
Computational domain thickness, δ	$5.895 \cdot 10^{-4}$ m	δ_b	30
Kinematic viscosity, γ	$4.75 \cdot 10^{-5}$ m^2/s	γ_b	0.4996
Inlet velocity, u	0.05~0.25 m/s	u_b	0.01~0.05
Inlet temperature, $T_{\rm in}$	873 K	T_{b1}	1
Outlet temperature, $T_{\rm out}$	773 K	T_{b2}	0.885

Code verification

In the simulation, the correctness of the model code is verified by comparing the calculated results of the LBM model with the analytical solution of the 3-D Poiseuille flow [23]. In the area with a grid number of 102 × 30 × 102, Re =-5 and, ω = 0.5, as shown in fig. 9. The fluid-flows into the structure along the direction parallel to the Y-axis, and the relative error is 4.2%.

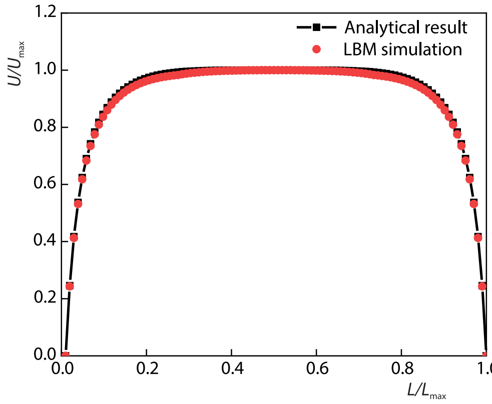

Figure 9. Comparison of analytical solution of 3-D Poiseuille flow and LBM calculation results

Results and discussion

Influence of ash layer on flow of DPF structure

Flow field analysis

The exhaust gas-flows into the porous medium structure along the Y-axis in a positive direction. Take the exhaust gas with inlet lattice velocity of 0.03 as an example. According to the theory of hydrodynamics, as the fluid-flows into the channel, its velocity increases accordingly. Due to the existence of porosity in the structure, there is no fluid passing through some positions of the structure. In Structures I and II, according to the comparison between figs. 10 and 11, it can be clearly found that the velocity field increases due to the decrease of porosity of the structure. According to the simulation results, the lattice velocity is obtained through the conversion coefficient, and the maximum value of the velocity field is increased from 0.310-0.313 m/s.

Effect of changing exhaust gas inlet velocity on DPF structure flow

The exhaust gase of 0.05 m/s, 0.10 m/s, 0.15 m/s, 0.20 m/s, and 0.25 m/s are, respectively introduced into the inlet of the structure. Due to the change of exhaust gas-flow rate at the inlet side, Reynolds number of the structure is 0.62, 1.24, 1.82, 2.48, and 3.10, respectively. Since the structure itself is a porous medium structure, the velocity inside the structure is uneven. Therefore, the average velocity, $u_{\rm mean}$, is introduced to represent the flow of porous media. As shown in fig. 12, under different Reynolds numbers of structures, the average velocity through the ash layered structure is less than the average velocity of the particle layers structure. With the increase of Reynolds number, the speed difference between them is greater. It is also confirmed that the porosity of ash layer is smaller than that of particle layers.

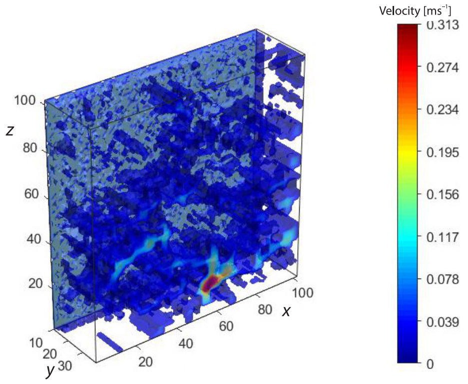

Figure 10. Velocity field without adding ash layer

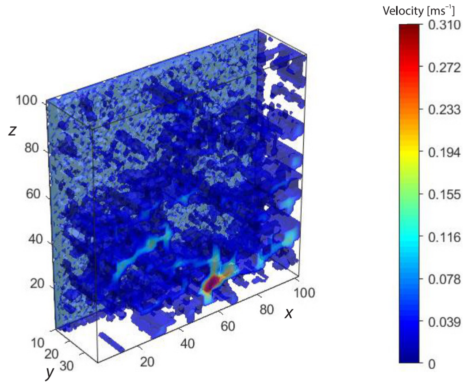

Figure 11. Velocity field with adding ash layer

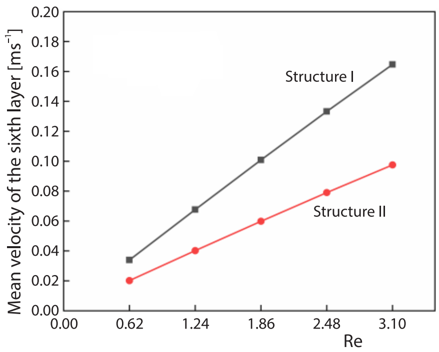

Figure 12. Relationship between average velocity of structure and Reynolds number

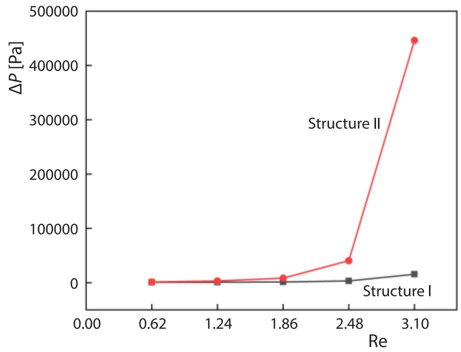

Figure 13. Relationship between inlet and outlet differential pressure Δ*P* and Reynolds number of structure

Effect of ash layer on pressure drop process of DPF structure

By changing the exhaust gas inlet velocity, the inlet and outlet differential pressure ΔP of the structure will also change accordingly. As shown in fig. 13. It can be found that by changing the gas inlet speed of the structure, the pressure difference gradually increases with the increase of the speed, and the pressure difference of the structure with ash layer is significantly greater than that of the structure without ash layer.

Influence of ash layer on heat transfer process of DPF structure

By simulating the change of temperature field before and after adding ash layer, the heat transfer process is from the first layer to the 30$^{\text{th}}$ layer, so the temperature distribution diagram of each layer of Structure I and II in the heat transfer process is obtained, as shown in figs. 14(a) and 14(b). By changing the inlet velocity of exhaust gas, its temperature field also increases with the increase of velocity. According to the law of conservation of energy, for Structure II with ash layer, the velocity field of fluid is greater than that of Structure I without ash layer. Therefore, the thermal energy of Structure II should be less than that of Structure I and the corresponding maximum temperature T_a should be greater than T_p.

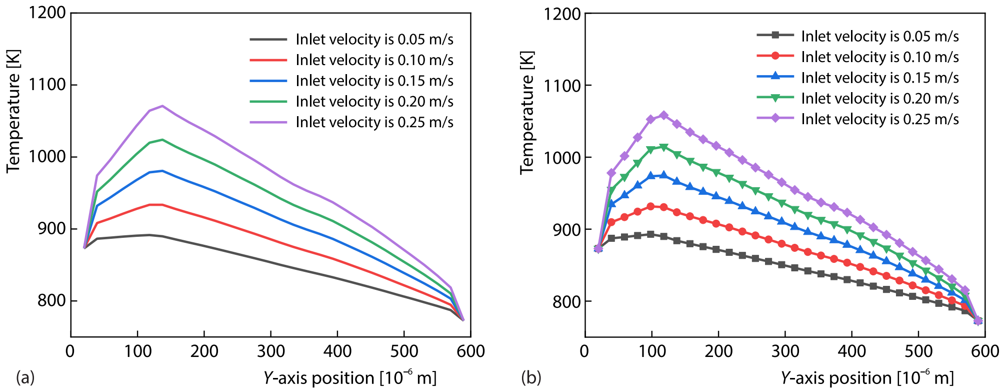

Figure 14. Temperature field of structure under the condition of changing velocity; (a) temperature field of Structure I and (b) temperature field of Structure II

Conclusions

In this paper, the porous micro-structures of ash layer, particle layer and DPF wall are established, and the influence of ash on the flow and heat transfer process of DPF is simulated using LBM method. Combined with the porosity, ε, and permeability coefficient, K, of ash layer and particle layer, it is found that the flow and heat transfer process of exhaust gas in the structure is complex. The results are as follows.

- The permeability coefficient of DPF micro-structure is $7.14 \cdot 10^{-12}$ m^2 calculated by Darcy's law. The permeability coefficients, K, of particle layer and ash layer on DPF surface are $4.13 \cdot 10^{-14}$ m^2 and $2.81 \cdot 10^{-13}$ m^2, respectively.
- When the exhaust gas-flows through the ash containing DPF structure, the velocity fields increase significantly. With the increase of Reynolds number, the average velocity difference between the ash layer and the particle layer is large. The porosity, ε, of the ash layer is small, which leads to the decrease of the velocity of passing through the ash layer. With the increase of exhaust gas velocity, the difference between the inlet and outlet pressure of ash containing DPF structure and that of the DPF structure without ash layer gradually increases, and the back pressure of ash containing DPF structure is higher.
- With the increase of flue gas inlet velocity, the heat transfer temperature of the structure also increases. The highest temperature point of fluid passing through Structure I moves forward than Structure II, and the highest temperature point of Structure I is greater than Structure II. This is of great guiding significance for the study of DPF particle regeneration process.

Acknowledgment

This work was supported by the National Science Foundation of China (52005149) and the Natural Science Foundation of Hebei Province (E2022202026).

Disclosure statement

No potential conflict of interest was reported by the author(s).

Nomenclature

C_P – constant pressure specific heat, [$Jkg^{-1}K^{-1}$]
e_α – discrete velocity
f_α – density distribution equation
f_α^{eq} – equilibrium density distribution equation
$\tilde{f}_\alpha$ – density distribution equation of collision step
$\tilde{g}_\alpha$ – temperature distribution equation of collision step
g_α – temperature distribution equation
g_α^{eq} – equilibrium temperature distribution equation
L – computational domain length, [m]
Pr – Prandtl number
P – physical pressure, [Pa]
ΔP – pressure difference, [Pa]
Re – Reynolds number ($=uL/v$)
T – temperature, [K]
T_p – temperature through the particle layer, [K]
T_a – temperature through ash layer, [K]
u – inlet velocity, [ms^{-1}]

Greek letters

α – thermal diffusion coefficient, [m^2s^{-1}]
γ – kinematic viscosity, [m^2s^{-1}]
δ – wall thickness, [m]
ε – porosity
λ – thermal conductivity, [$Wm^{-1}s^{-1}$]
μ – dynamic viscosity, [$kgm^{-1}s^{-1}$]
ρ – density, [kgm^{-3}]
τ – dimensionless relaxation time

Acronyms

BGK – Boltzmann-Bhatnagar, Gross and Krook
D_3Q_{19} – the 3-D nineteen-velocity lattice model
DPF – diesel particulate filter
LBM – lattice Boltzmann method
QSGS – quartet structure generation set

References

[1] Lloyd, A. C., *et al*., Diesel Engines: Environmental Impact and Control, *Journal of the Air and Waste Management Association*, *51* (2001), 6, pp. 809-847
[2] Rhys-Tyler, G. A., *et al*., The Significance of Vehicle Emissions Standards for Levels of Exhaust Pollution from Light Vehicles in An Urban Area, *Atmospheric Environment*, *45* (2011), 19, pp. 3286-3293
[3] Sappok, A., *et al*., Ash Effects on Diesel Particulate Filter Pressure Drop Sensitivity to Soot and Implications for Regeneration Frequency and DPF Control, *SAE International Journal of Fuels and Lubricants*, *3* (2010), 1, pp. 380-396
[4] Wang, H., *et al*., Ash Deposited in Die*sel Particular Filter: A Review, Energy Sources – Part A: Recovery,* Utilization, and Environmental Effects, *41* (2019), 18, pp. 2184-2193
[5] Song, C., *et al*., Carbonyl Compound Emissions from a Heavy-Duty Diesel Engine Fueled with Diesel Fuel and Ethanol-Diesel Blend, *Chemosphere*, *79* (2010), 11, pp. 1033-1039
[6] Bai, S., *et al*., Influence of Active Control Strategies on Exhaust Thermal Management for Diesel Particular Filter Active Regeneration, *Applied Thermal Engineering*, *119* (2017), June, pp. 297-303
[7] Giechaskiel, B., *et al*., Engine Exhaust Solid sub-23 nm Particulates: II, Feasibility Study for Particulate Number Measurement Systems, *SAE International Journal of Fuels and Lubricants*, *7* (2014), 3, pp. 935-949
[8] Wang, H., *et al*., Pore Morphology and Fractal Dimension of Ash Deposited in Catalyst Diesel Particulate Filter, *Environmental Science and Pollution Research*, *27* (2020), 10, pp. 11026-11037
[9] Gao, J. B., *et al*., A Review of Fundamental Factors Affecting Diesel PM Oxidation Behaviors, *Science China Technological Sciences*, *61* (2018), 3, pp. 330-345
[10] Fu, J., *et al.*, Four Kinds of the Two-Equation Turbulence Model's Research on Flow Field Simulation Performance of DPF's Porous Media and Swirl-Type Regeneration Burner, *Applied Thermal Engineering*, *93* (2016), Jan., pp. 397-404
[11] Mohamad, A. A., *Lattice Boltzmann Method*, Springer, London, UK, 2011
[12] Yamamoto, K., *et al*., Simulation on Soot Deposition and Combustion in Diesel Particulate Filter, *Proceedings of the Combustion Institute*, *32* (2009), 2, pp. 1965-1972
[13] Yamamoto, K., *et al*., Simulation on Catalytic Reaction in Diesel Particulate Filter, *Catalysis Today*, *153* (2010), 3-4, pp. 118-124
[14] Yamamoto, K., *et al*., Simulation of Heat Conduction and Soot Combustion in Diesel Particulate Filter, *Progress in Computational Fluid Dynamics, an International Journal*, *12* (2012), 4, pp. 286-292
[15] Yamamoto, K., *et al*., Simulation of Continuously Regenerating Trap with Catalyzed DPF, *Catalysis Today*, *242* (2015), Part B, pp. 357-362
[16] Li, Z., *et al*., Simulation of Soot Particulate Deposition Inside Porous Walls Based on Lattice Boltzmann Method for Diesel Particulate Filter, *Journal of Environmental Chemical Engineering*, *9* (2021), 4, 105396

[17] Hu, X., *et al.*, Analysis of Boundary Conditions for Lattice Boltzmann Model, *Journal of Hydrodynamics*, (2003), 2, pp. 127-134
[18] Meng, Z., *et al*., Effect of Particulate Characteristics on DPF Regeneration Performance, *Journal of Combustion Science and Technology*, *24* (2018), 2, pp. 186-191
[19] Yang, J., *et al*., Single Wall Diesel Particulate Filter (DPF) Filtration Efficiency Studies Using Laboratory Generated Particulates, *Chemical Engineering Science*, *64* (2009), 8, pp. 1625-1634
[20] Ou, J., *et al*., Experimental Investigation on the Variation Characteristics of Soot Layer Thickness and Pressure Drop during DPF/CDPF Active Regeneration, *Chemical Engineering Science*, *241* (2021), 116682
[21] Meng, Z., *et al*., Experimental Study on the Influence of DPF Micro-Pore Structure and Particle Property on its Filtration Process, *Journal of Combustion*, *2016* (2016), ID9612856
[22] Cho, H., *et al*., Permeability of Micro-Scale Fibrous Porous Media Using the Lattice Boltzmann method, *International Journal of Heat and Fluid-Flow*, *44* (2013), Dec., pp. 435-443
[23] Kitao, T., *et al*., Validation of LBM Simulation of Saturated Seepage Flow through 3-D-Printed Homogeneous Porous Medium for Fluid-Particle Coupled Analysis, *Acta Geotechnica*, *16* (2021), 8, pp. 2643-2656

Paper submitted: November 9, 2022
Paper revised: January 4, 2023
Paper accepted: January 6, 2023